Title

Single crystals of mechanically entwined helical covalent polymers

Journal

Nature Chemistry, 13(7)

ISSN

1755-4330

Authors

Hu, Yiming

Teat, Simon J

Gong, Wei

et al.

Publication Date

2021-07-01

DOI

10.1038/s41557-021-00686-2

Peer reviewed

Single-Crystal Mechanically Entwined Helical Covalent Polymer

Yiming Hu[1], Simon J. Teat[2], Wei Gong[3], Zhou Zhou[4], Yinghua Jin[1], Hongxuan Chen[1], Jingyi Wu[1], Yong Cui[3], Tao Jiang[4], Xinbin Cheng[4], Wei Zhang[1]*

[1]Department of Chemistry, University of Colorado Boulder, Boulder, CO 80309, USA

[2]Advanced Light Source, Lawrence Berkeley National Laboratory, Berkeley, CA 94720, USA

[3]School of Chemistry and Chemical Engineering, Frontiers Science Center for Transformative Molecules and State Key Laboratory of Metal Matrix Composites, Shanghai Jiao Tong University, Shanghai 200240, China

[4]MOE Key Laboratory of Advanced Micro-Structured Materials and School of Physics Science and Engineering, Tongji University, Shanghai 200092, China

*Email: wei.zhang@colorado.edu

Abstract

Helical covalent polymers (HCPs) have long been fascinating to scientists in a broad range of disciplines from biology to materials science. However, due to their grand synthetic challenge, single crystal structures of HCPs with high molecular weight and precise atomic positions, bond lengths and angles have never been obtained. Herein, we report a chiral single crystal structure of a HCP taking double helix conformation. The structure analysis shows that each duplex is mechanically entwined and stabilized by the hydrogen-bonding interactions with neighboring duplexes, forming an extended three-dimensional network. Such unprecedented chemical-mechanical hybrid bonding approach would open many new possibilities for the design and synthesis of higher order functional polymeric architectures, including double helix polymers and their assemblies.

The discovery of the double helix structure of deoxyribonucleic acid (DNA) by Watson and Crick has been one of the most significant scientific achievements of all time[1]. The elegant pairing of two DNA strands, its mode of complementary chain reproduction, and the encoded hereditary information have inspired and challenged many scientists. Chemists have been trying to build molecules that can rival the sophistication of nature's biomacromolecules. Tremendous progress has been made in building single-stranded helical structures with a broad structural diversity from small molecule assemblies[2], foldamers (oligomers)[3,4] to larger polymers[5,6]. Synthetic helical oligomers/polymers have mainly been characterized using solution phase techniques, such as NMR spectroscopy, circular dichroism (CD) spectroscopy, optical rotation, etc. Uniaxially oriented fibers and films of helical polymers have been prepared to elucidate their solid phase structural information through X-ray diffraction (XRD) analysis and microscopic observations, such as atomic force microscopy (AFM) and scanning tunneling microscopy (STM)[7-12]. However, structural details of synthetic helical polymers have rarely been revealed at atomic resolution through single crystal X-ray diffraction (SCXRD) analysis, due to the extreme difficulty in obtaining single crystals.

Further assemblies of single strands to higher-order multistrand helices, which are widely observed in proteins and DNAs[13], have been extremely challenging to achieve even with abiotic polymers[14]. The study on synthetic double helices has mainly been limited to short helical oligomers. One such example is the seminal work by Lehn on the dimerization of oligopyridinecarboxamides with bent conformations to form double-stranded helices through intramolecular hydrogen bonding and intermolecular aromatic stacking interactions[15,16]. More recently, Yashima reported an enantiomeric double-stranded helicate, where hexa(*m*-phenylene)s equipped with phenol groups are dimerized through the formation of spiroborate bridges[17,18]. These short double helices are soluble in organic solvents and their structures have been thoroughly investigated through various solution phase characterizations as well as single

crystal X-ray diffraction analyses, providing valuable insights into the fundamental structure properties of double helices. High molecular weight synthetic polymers that form long double helices are very rare and single crystal structures of such polymers have never been obtained[19,20]. As a result, the direct observation of precise atomic positions and bond lengths and angles in double helical polymers has been impossible, and folding, winding, and further self-assembly mechanisms remain elusive. Moreover, the only strategy of forming double helices over the past three decades has been maneuvering secondary attractive interactions between the two single-stranded subunits.

Herein, we report an unprecedented chiral single crystal structure of a linear covalent polymer (number of repeating units = 4×10^4) taking a double helix conformation. The single crystal structure analysis shows that, unlike any natural biopolymers, the two strands of the double helix are mechanically entwined without noticeable non-covalent interactions between them. Rather, each helical strand is stabilized by the hydrogen-bonding interactions with a neighboring double helix, forming an extended network of double helices. Such previously unrevealed topology and intertwining mechanism of a helical polymer somewhat reminds us of the famous allegory of the Long Spoons, showing enthralling interdependence between double helices. We propose that our system may offer an alternative working model to study the relationship between the structures of linear polymers and their potential to arrange into a double helix. Moreover, the chemical-mechanical hybrid bonding approach reported herein would open many new possibilities for the design and synthesis of higher order functional polymeric architectures, including double helix polymers and their assemblies.

Results and discussion

We synthesized the helical covalent polymer (**HCP**) through condensation reaction of 2,3,6,7,10,11-hexahydroxytriphenylene (HHTP) with $B(OMe)_3$ in the presence of LiOH (Fig. 1a). Initially, we tried the well-known condensation of HHTP with $B(OH)_3$ in DMF to form spiroborate linked polymers. However, even after heating at 120 °C for 3 days, we only obtained a gel-like material that is soluble in acetone.

Presumably, low molecular weight oligomers were formed. We then screened various reaction conditions, such as solvents (MeOH, H_2O, *o*-dichlorobenzene, THF, pyridine, DMF, DMSO, and nitrobenzene), boronic acid derivatives ($B(OH)_3$ and $B(OMe)_3$), and bases (LiOH, NaOH, DMF). We found the crystalline product can be obtained when HHTP was reacted with $B(OMe)_3$ in nitrobenzene in the presence of LiOH. Large single crystals were obtained in elongated square bipyramid shape with an average size of 20 to 30 μm (the distance between the two pyramid apexes) as shown in optical microscopy (Fig. 1b) and Scanning Electron Microscopy (SEM) images. The structure of the product was characterized by FT-IR, ^{13}C, ^{11}B, ^{7}Li solid-state nuclear magnetic resonance (NMR) spectroscopy, and single-crystal X-ray diffraction analysis. Surprisingly, although theoretically 2D covalent organic framework (COF) structure can be formed from 2:3 molar ratio of HHTP and $B(OMe)_3$ by fully converting all the diols to spiroborate linkages under the applied solvothermal conditions, only two pairs of diols of HHTP reacted, forming the zig-zag shaped polymer chains with one unreacted diol group. The formation of the unusual helical backbone can be attributed to the multitude hydrogen bond interactions found between the unreacted diols and spiroborate units, which provide energy gain and stabilization. The reduced symmetry of the HHTP monomer units leads to nonequivalent aromatic carbons, which is consistent with the resonance peaks observed in the ^{13}C NMR spectrum (Fig. 1c).

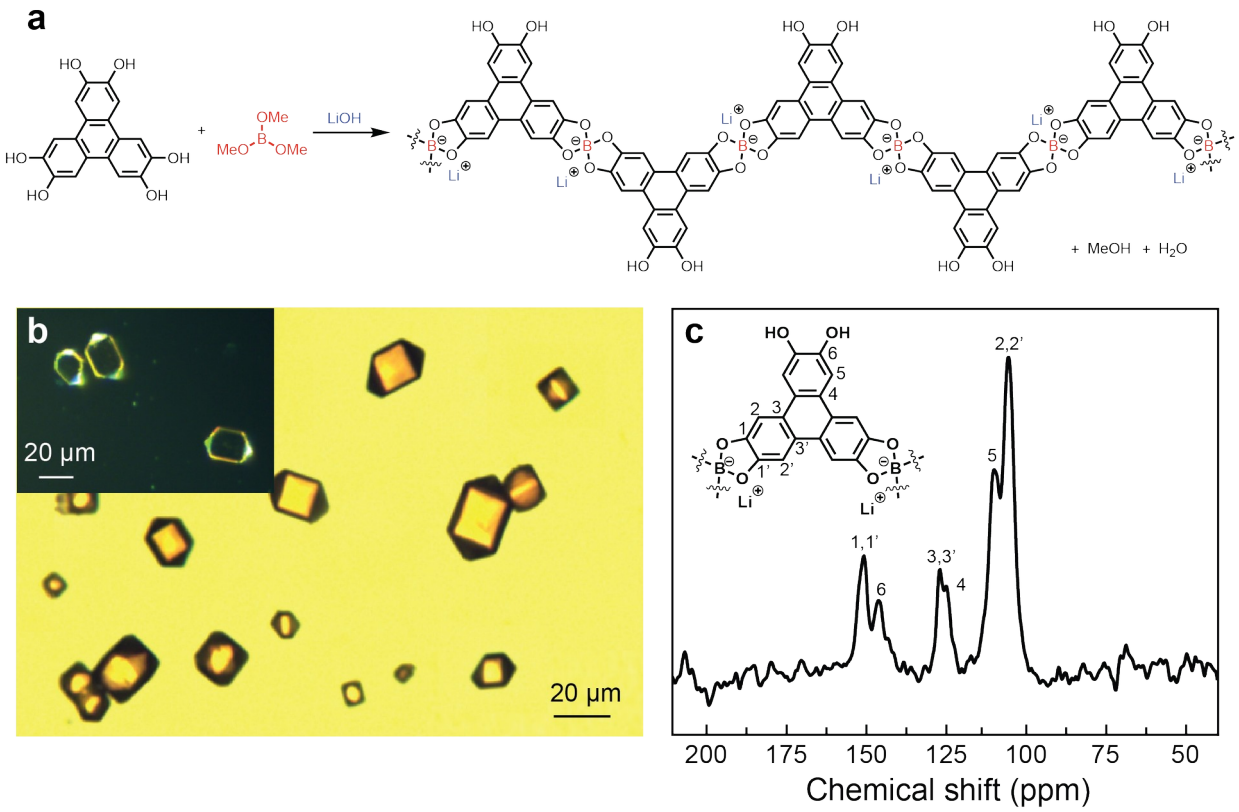

Figure 1 | Helical Covalent Polymer (HCP). a, Synthesis of the helical polymer through spiroborate formation. **b**, Optical images of the large single crystals of the **HCP**. The **HCP** grew in elongated square bipyramid shapes. Inset in b, a dark-field optical microscope image with high contrast at edges. **c**, Solid-state ^{13}C NMR spectrum of the **HCP**. Two sets of resonance peaks were observed, corresponding to non-equivalent aromatic carbons in the polymer structure.

The linear polymer has a high degree of polymerization ($n = 4 \times 10^4$) and a molecular weight of 1.3×10^7 Da. for a single strand, which, to the best of our knowledge, represents the largest crystalline purely covalent helical polymer reported thus far. The double helical structure of the **HCP** was unambiguously determined by single-crystal X-ray diffraction with discrepancy factor *R* of 7.80%. Previously unresolved structural information regarding to polymer helicity, such as exact atomic positions and geometric parameters (bond lengths and angles), helical pitch, helical conformation, and 3D packing are clearly revealed for the first time. The **HCP** crystallized in the Orthorhombic *I*222 space group with lattice

constants, a = 15.2487(11) Å, b = 19.3901(11) Å and c = 19.4093(12) Å with one whole formula unit in the asymmetric unit. Two adjacent HHTP monomers linked by a spiroborate $[BO_4]^-$ node are twisted with respect to each other at a dihedral angle of 66°, thus forming an infinite helical chain along the a-axis, which is assembled by spirals along the a direction requiring 2 unit cells and 4 formula units to complete one full rotation (Fig. 2a). Each unit cell is composed of helical strands with the same chirality. The two strands shift 15.2 Å along the a-axis with respect to each other to form double-stranded helices. Four HHTP monomers make a complete turn (corresponding to 90° rotation per residue) with a helical pitch of 30.50 Å. (Fig. 2b). Considerable distortion of the $[BO_4]^-$ group was observed, where the dihedral angle of $[BO_4]^-$ changes from more common 90˚ to 66˚ (Fig. 2a). These bond deformations provide the optimum geometry of the polymer chain to form a 1/5 helix, which requires a dihedral angle of 66° between monomers with the internal angle of 120°. We believe the high conformational adaptability of the spiroborate linkage is playing a critical role in forming the observed double helix conformation, which further induces the crystallization in a chiral space group.

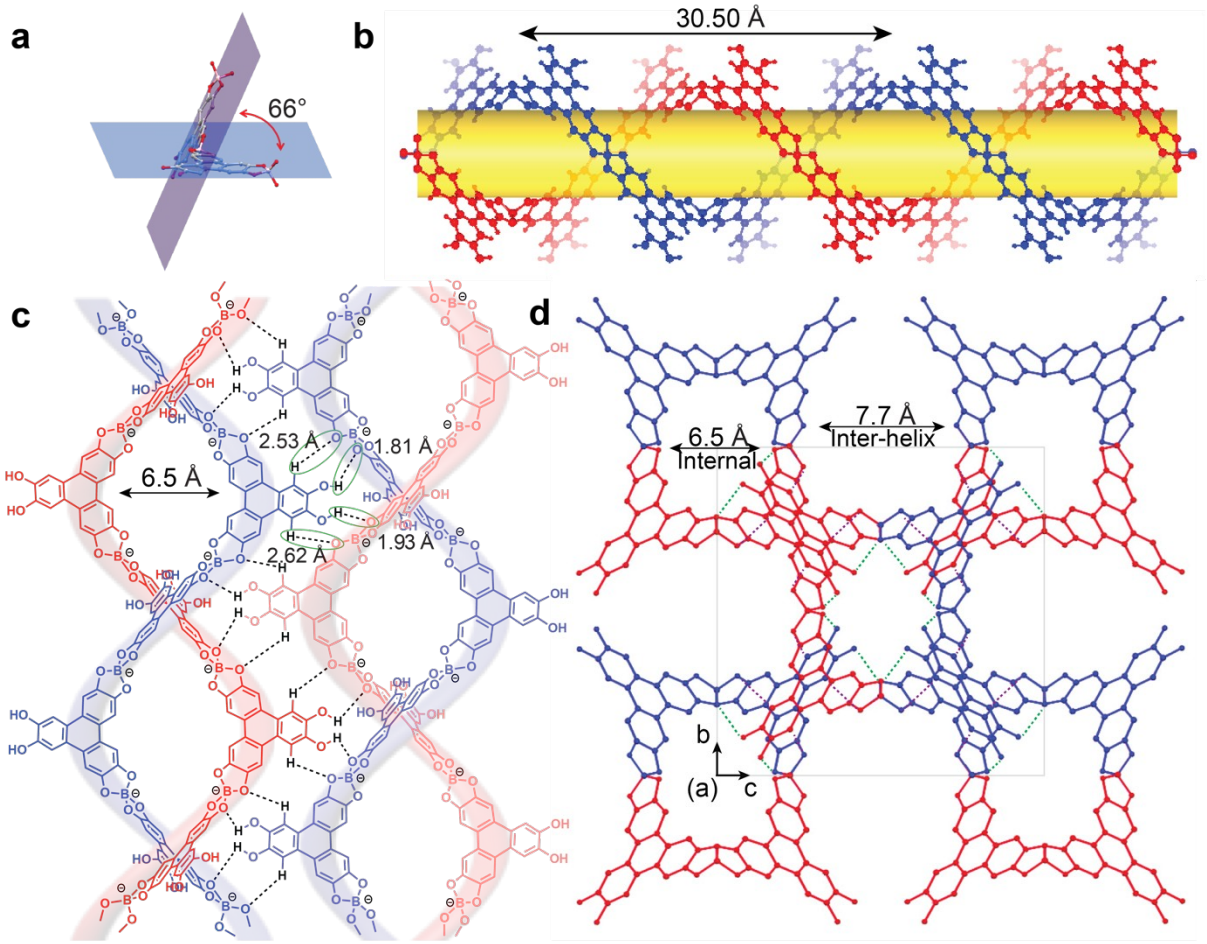

Figure 2 | Single crystal structures of the HCP showing double helical conformation. a, The backbone twisting geometry to form helical conformation. The $[BO_4]^-$ linkages are distorted and the dihedral angle between two HHTP monomers is 66°. **b**, The stick representation of a double helix along the *b* axis. The two strands are color-coded for clarity. Each helical pitch, the height of one complete turn (360°), is 30.50 Å long. Four HHTP monomer units with the internal angle of 120° are needed per turn. No strong interactions are present between the monomer units of the same strand. **c**, Formation of double helices through an array of hydrogen bonding interactions along the *a*-axis. The closest inter-strand distance within one double helix is measured from Ar-H to H-Ar (6.5 Å). The formation of double-stranded helices is guided by the hydrogen bonding interactions (strong, OH···O-B-O; weak Ar-H···O-B-O) with neighboring double helices. **d**, The view along the a axis showing the interdependence of double

helices and two types of square cavities. The H-bonding interactions of the central helix with the eight strands of the surrounding four double helices are shown. The complete turn of the single strand is supported by 16 strong OH···O-B-O H-bonding interactions (green dot line) and 16 weak Ar-H···O-B-O H-bonding interactions (violet dot line) with the four sets of neighboring double helices. The diameters of the internal and inter-duplex cavity are defined as the closest distances between the two ArH hydrogen atoms (6.5 Å) of the opposite strands for the former and between the two $[BO_4]^-$ oxygen atoms (7.7 Å) of the opposite strands for the latter.

There are no strong interactions and stabilization within the same strand or between the two strands of the same double helix. The shortest inter-strand distance between the backbones of the two strands of a duplex is 6.5 Å, which is beyond the effective range (0.6 nm) of common van der Waals interactions. Instead, the conformational stability of the helical strands and their intertwining into double helices are assisted by the hydrogen bonding interactions between adjacent duplexes (Fig. 2c). The unreacted diol groups of each strand orient in a way to induce strong hydrogen bonding interactions (OH···O-B-O distance of 1.81-1.93 Å) with the $[BO_4]^-$ groups of the neighboring double helix. The duplex stability is further enhanced by the weak hydrogen bonding interactions (Ar-H···O-B-O distance of 2.53-2.62 Å) between Ar-H and the oxygens of the $[BO_4]^-$ groups at the interface of two duplexes. Each repeating unit provides four oxygens of $[BO_4]^-$ group as H-bond acceptors and two OH groups and two Ar-H moieties as H-bond donors. Therefore, each complete turn of a single strand is stabilized by 16 strong OH···O-B-O hydrogen-bonding interactions and 16 moderate Ar-H···O-B-O hydrogen-bonding interactions with neighboring four sets of double helices.

Such interdependence of double helices gives rise to an unusual helical topology, where the double helix formation is mainly guided by neighboring four double helices, resulting in an extended 3D network structure. This type of topology is distinct from DNA-like double helical tertiary structure in which inter-strand H-bonding interactions within a double helix provide the main stabilization. When viewed in

projection down the *a* axis, the helices appear to have a cross section consisting of two types of square channels, one from the internal cavity of a double helix (diameter of 6.5 Å) and the other from inter-helix cavity (diameter of 7.7 Å) as shown in Fig. 2d. The stabilization of each double helix by the neighbors is much like the setting in the parable of the long spoons: Survival through Sharing.

The double helical conformation of such polymer chains and their compact packing along the *a* axis result in high-density linear alignment of the charged species along the walls of the channels. One spiroborate anion is located at every 15.2 Å along the helical axis and ~ 9.5 Å perpendicular to the helical axis at all equivalent positions in the unit cell. The rigid backbone structure and peculiar topology of the double helices in turn provide channels with a highly packed charge distribution. The lithium counter-ions are hosted in the central square tubular cavity surrounded by four double helices. The densely charged columnar channels with a high stiffness could potentially mediate cation migration along the wire with high efficiency.

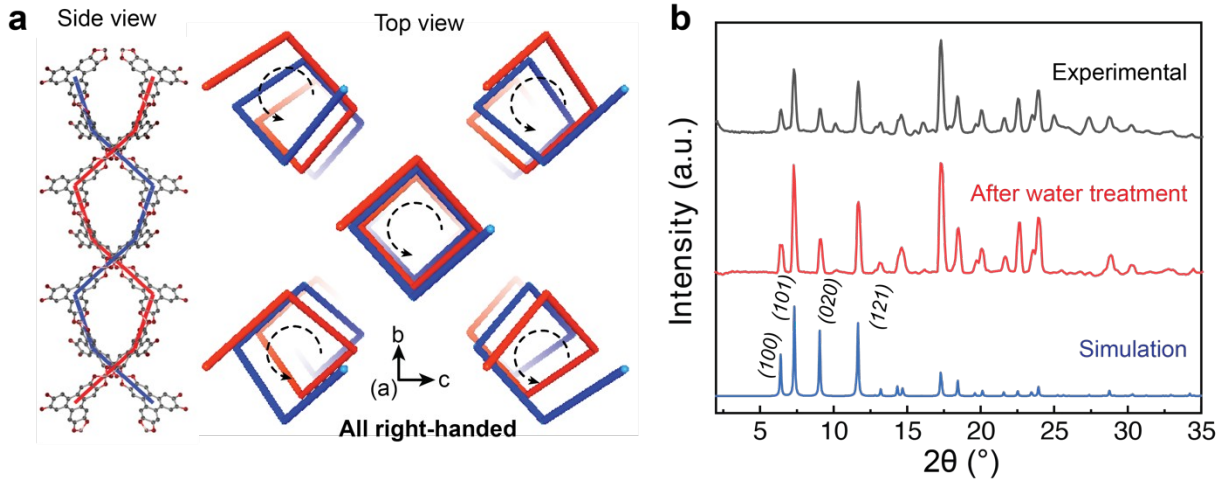

Figure 3 | HCP helical chirality and PXRD patterns. a, left, side view of one double helix unit, the backbone was colored for visualization; right, top view along *a* axis of **HCP** double helix structure. All double helices show the same right-handed chirality[21]. **b**, The simulated PXRD patterns from the single crystal diffraction data match well with the experimental results of the bulk sample. The crystals of **HCP**

have high water stability. The PXRD patterns of the water treated sample (soaking in water for 48 h) remain identical to those of the pristine sample.

We examined the X-ray diffraction patterns of multiple single crystals and found only single-handed helical polymers are present in one crystal domain (Fig. 3a). Our observation is in great contrast to the isotactic poly(methyl methacrylate) double helices, where the double stranded helices of right-handed and left-handed senses pack together in the unit cell to form hexagonal-like closest packing mode[20]. In a more recent example, Yaghi and coworkers also reported the synthesis of overall racemic three-dimensional covalent organic framework (COF-505), where achiral monomers form helical organic threads of opposite chirality in one crystalline domain[22]. While optically active double helices are common in nature, they are rarely observed in achiral synthetic macromolecules. We attribute the formation of enantiomorphic crystals from the achiral HHTP monomers to the combined effect of the following factors: (i) Initial generation of chirality by helical arrangement of the monomers. The helical chirality evolves when 4-mer makes a complete turn. (ii) The single strand chiral oligomers bundle with other geometry matching helices to form stable nuclei. This process involves stabilization of the single strands through cooperative supramolecular hydrogen bonding interactions with helices that have matching geometry (i.e. the same helicity)[23]. Each helical strand interacts with four neighboring helices (two sets of double helices) through multiple hydrogen bonding interactions (total eight hydrogen bonds per monomer unit), forming double helices and their supramolecular aggregates. As there are no close interactions between two strands of the same double helix, it is unlikely that double helices form before nucleation. (iii) Subsequent growth of the nuclei into 3D crystal structures occurs through continuous addition of the monomers in crystallographically aligned direction. The positioning of the monomers, crystal growth direction, and chirality are likely controlled by the energy landscape at the interface of the monomers and crystalizing nuclei. Geometry mismatch between the monomers and the nucleus would cause energy penalties due to the difference in hydrogen bonding stabilization and a strain-energy contribution. In this

context, the dynamic nature of spiroborate linkages and hydrogen bonding is critical, which enables error correction. Enantiomorphic single crystals are formed through the strong cooperative response (inter-helical hydrogen bonding) between single strands and balancing the rate of polymerization and crystallization. Such chiral polymer growth mechanism is similar to nucleation and growth mechanism of crystalline covalent organic frameworks (COFs), where monomers polymerize and crystalize in specific favored orientations through reversible self-addition polymerization to form highly periodic networks[24-26]. Although individual crystals contain only one type of chiral helices, the CD characterization of the bulk crystal sample shows racemic conglomerate, indicating an equal amount of right-handed and left-handed crystals are present. Therefore, there is no initial preference on the formation of left-handed and right-handed oligomers, and the symmetry breaking likely occurs during the crystallization process.

To confirm the phase purity of the **HCP** single crystals, powder X-ray diffraction (PXRD) measurement was conducted with the bulk sample (Fig. 3b). The experimental PXRD patterns of the bulk sample closely match the calculated powder diffraction patterns of the single crystal structure, indicating only a single phase is present. The crystalline structure of the **HCP** is highly stable in water, remaining intact even after soaking in water for 48 hours at room temperature. The PXRD diffraction of the sample after water treatment is almost identical to the fresh sample, confirming that the crystallinity of the helical polymer fully retains under the hydrolysis condition. The crystallinity of the sample retains even after removal of the solvent under high vacuum at 80 °C (Supplementary Fig. 11, and 12). The high stability of the double helices and their packing structure is attributed to the stability of the spiroborate groups and a collection of H-bonding interactions acting between the neighboring double helices, reminiscent of DNA base-pairing.

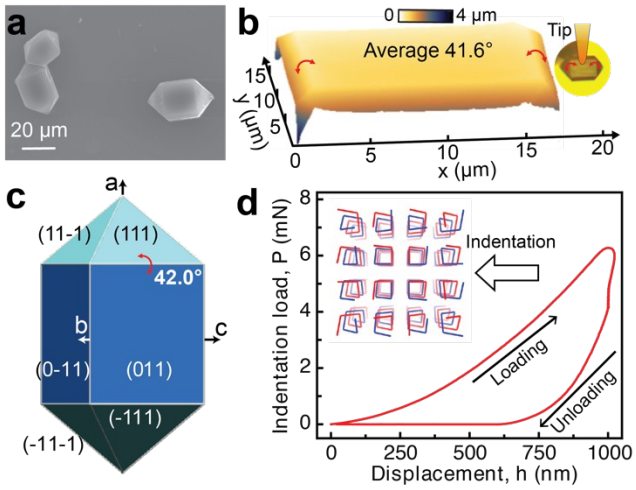

Figure 4 | HCP morphology and mechanical property. a, SEM image of the single crystal **HCP**. **b**, AFM image of **HCP**. Inset: optical microscopy of the measured crystal surface. **c**, Proposed model of single crystal **HCP**. **d**, The typical load-displacement curve (*P*–*h*) of the cubic face of the single crystal. The average elastic modulus was measured to be E = 5.5 GPa. Inset: the indentation direction toward {0, 1, 1} facet.

According to the unit cell, the crystal adopts an orthorhombic crystal system with very close cell-edge lengths along the *b* and *c* axes (*b* = 19.3901 Å and *c* = 19.4093 Å). Therefore, a near square projection was expected in the *bc* plane, perpendicular to the *a* axis. In the SEM figure (Fig. 4a) and optical microscopy, all the crystals show similar morphology, a cuboid covered with two pyramids on the opposite faces. For some of the crystals, a near square projection can be observed. Based on these observations and unit cell parameters, the morphology model was proposed as shown in fig. 4c, where the {1, 1, 1}, {-1, 1, 1} and {0, 1, 1} facets were applied to build a closed polyhedron. Interfacial angles are of crucial importance to studying a crystal with a definite geometric shape. Thus, the angle between two major faces, the triangle and rectangle, was measured by AFM. The AFM images clearly show the multiple planes of each crystal and the interfacial angles between the neighboring planes. It should be noted that the residue left after the solvent drying caused the roughness in the AFM topography. We extracted all the angles between {0, 1, 1} facets and{1, 1, 1} as well as {-1, 1, 1} (Supplementary Fig. 5

and Supplementary Fig. 6) and found that the average interfacial angles value of 41.6° agrees well with the simulated value of 42.0°.

The preliminary investigation of mechanical properties of the **HCP** single crystal was conducted using three-sided pyramid indenters to measure the modulus of elasticity and hardness of a selected crystallographic plane. We were able to perform nanoindentation with a Berkovich indenter on the large rectangular surface, which was identified as {0, 1, 1} facet. The surface profile of the {0, 1, 1} facet was obtained using AFM, which shows the uniform thickness and smoothness (Fig. 4b). From load–displacement relationships (*P*–*h* curves), the average elastic modulus was estimated to be 5.5 GPa. It should be emphasized that the external force was applied on {0, 1, 1} facet, and the measured mechanical strength primarily results from the inter-helical H-bonding interactions without any covalent bonding.

Conclusion

We demonstrated how a simple achiral monomer can self-organize into chiral single crystals of double-helical polymers by harnessing distinct covalent and supramolecular interactions. The chemical-mechanical hybrid bonding approach reported herein would open many new possibilities for the design and synthesis of well-defined functional molecular and polymeric architectures, and also suggests novel platforms for linear polymer folding, supramolecular intertwining, and chirality propagation. Moreover, the anisotropy of electric and mechanical properties of the highly-charged, infinitely long helical polymer crystals could be exploited for the future development of novel materials and nanosystems with functions beyond native biopolymers and biosystems.

Methods:

Synthesis and crystallization of HCP

The helical covalent polymer was prepared by tetraborate condensation reaction of HHTP, LiOH and $B(OMe)_3$ in nitrobenzene in ampoules tube. A 5 mL tube was charged with HHTP (32.4 mg, 0.1 mmol),

LiOH (power form, 3.6 mg, 0.15 mmol) and a tiny stir bar (Size: 10 x 3 mm), then $B(OMe)_3$ (17 μL, 0.15 mmol) dissolved in nitrobenzene (3 mL) were added. The tube was frozen at 77 K in the liquid nitrogen bath for 2 min, then evacuated and refilled with N_2 for 3 cycles, and finally sealed with open flame at a pressure around 100 mTorr. The sealed tube was warmed up at room temperature and then placed at the center of the stir plate with a stirring speed at 100 rpm at 80 °C for 12 hours. The tube was then placed in the oven (120 °C) for 30 days without disturbance. It is necessary to stir the mixture initially to dissolve all LiOH powder. When the mixture was directly heated at 120 °C without stirring at the beginning of the reaction, we observed a large amount of unreacted LiOH crystals covered by the product, leading to the low conversion. After the reaction, the crystals (20 to 30 μm) were collected by vacuum filtration, washed with acetone, methanol and dried under vacuum. The product was further washed with THF through Soxhlet extraction method (24 h) to provide helical covalent polymer (15.5 mg, 46%). The optical microscopy, SEM, Single-crystal XRD, and nano-indentation were carried out with crude suspension after gentle sonication.

Crystallographic data deposition

Crystal data for the two HCP crystals (tentatively assigned to right-handed) are available from the Cambridge Crystallographic Data Centre via www.ccdc.cam.ac.uk (CCDC 2017159, 2034057).

References

1 Watson, J. D. & Crick, F. H. C. Molecular Structure of Nucleic Acids: A Structure for Deoxyribose Nucleic Acid. *Nature* **171**, 737-738, (1953).

2 Yashima, E. *et al.* Supramolecular Helical Systems: Helical Assemblies of Small Molecules, Foldamers, and Polymers with Chiral Amplification and Their Functions. *Chem. Rev.* **116**, 13752-13990, (2016).

3 Hill, D. J., Mio, M. J., Prince, R. B., Hughes, T. S. & Moore, J. S. A Field Guide to Foldamers. *Chem. Rev.* **101**, 3893-4012, (2001).

4 Zhang, D.-W., Zhao, X., Hou, J.-L. & Li, Z.-T. Aromatic Amide Foldamers: Structures, Properties, and Functions. *Chem. Rev.* **112**, 5271-5316, (2012).

5 Nakano, T. & Okamoto, Y. Synthetic Helical Polymers: Conformation and Function. *Chem. Rev.* **101**, 4013-4038, (2001).

6 Yashima, E., Maeda, K., Iida, H., Furusho, Y. & Nagai, K. Helical Polymers: Synthesis, Structures, and Functions. *Chem. Rev.* **109**, 6102-6211, (2009).

7 Percec, V. *et al.* Steric communication of chiral information observed in dendronized polyacetylenes. *J. Am. Chem. Soc.* **128**, 16365-16372, (2006).

8 Percec, V. *et al.* Self-Assembling Phenylpropyl Ether Dendronized Helical Polyphenylacetylenes. *Chem. Eur. J.* **13**, 9572-9581, (2007).

9 Percec, V. *et al.* Synthesis, structural, and retrostructural analysis of helical dendronized poly (1-naphthylacetylene) s. *J. Polym. Sci. Pol. Chem.* **45**, 4974-4987, (2007).

10 Rudick, J. G. & Percec, V. Nanomechanical function made possible by suppressing structural transformations of polyarylacetylenes. *Macromol. Chem. Phys.* **209**, 1759-1768, (2008).

11 Motoshige, A., Mawatari, Y., Motoshige, R., Yoshida, Y. & Tabata, M. Contracted helix to stretched helix Rearrangement of an aromatic polyacetylene prepared in n-hexane with [Rh (norbornadiene) Cl] 2-triethylamine catalyst. *J. Polym. Sci. Pol. Chem.* **51**, 5177-5183, (2013).

12 Liu, X.-Q., Wang, J., Yang, S. & Chen, E.-Q. Self-organized columnar phase of side-chain liquid crystalline polymers: to precisely control the number of chains bundled in a supramolecular column. *ACS Macro Lett.* **3**, 834-838, (2014).

13 Baker, D. A surprising simplicity to protein folding. *Nature* **405**, 39-42, (2000).

14 De, S. *et al.* Designing cooperatively folded abiotic uni-and multimolecular helix bundles. *Nat. chem.* **10**, 51, (2018).

15 Lehn, J.-M. *et al.* Spontaneous assembly of double-stranded helicates from oligobipyridine ligands and copper (I) cations: structure of an inorganic double helix. *Proc. Natl. Acad. Sci. U.S.A.* **84**, 2565-2569, (1987).

16 Berl, V., Huc, I., Khoury, R. G., Krische, M. J. & Lehn, J.-M. Interconversion of single and double helices formed from synthetic molecular strands. *Nature* **407**, 720-723, (2000).

17 Miwa, K., Furusho, Y. & Yashima, E. Ion-triggered spring-like motion of a double helicate accompanied by anisotropic twisting. *Nat. Chem.* **2**, 444-449, (2010).

18 Ousaka, N. *et al.* Spiroborate-based double-stranded helicates: meso-to-racemo isomerization and ion-triggered springlike motion of the racemo-helicate. *J. Am. Chem. Soc.* **140**, 17027-17039, (2018).

19 Wang, Y. *et al.* Double helical conformation and extreme rigidity in a rodlike polyelectrolyte. *Nat. Commun.* **10**, 1-8, (2019).

20 Kusanagi, H., Chatani, Y. & Tadokoro, H. The crystal structure of isotactic poly (methyl methacrylate): packing-mode of double stranded helices. *Polymer* **35**, 2028-2039, (1994).

21 Due to the wavelength of the data collections and all light element compositions of HCP, the assignment of the absolute handedness of the individual crystals was challenging. We tentatively assigned the handedness of the presented crystal structure to right-handed.
22 Liu, Y. *et al.* Weaving of organic threads into a crystalline covalent organic framework. *Science* **351**, 365-369, (2016).
23 Leiras, S., Freire, F., Quiñoá, E. & Riguera, R. Reversible assembly of enantiomeric helical polymers: from fibers to gels. *Chem. Sci.* **6**, 246-253, (2015).
24 Beaudoin, D., Maris, T. & Wuest, J. D. Constructing monocrystalline covalent organic networks by polymerization. *Nat. Chem.* **5**, 830-834, (2013).
25 Evans, A. M. *et al.* Seeded growth of single-crystal two-dimensional covalent organic frameworks. *Science* **361**, 52-57, (2018).
26 Ma, T. *et al.* Single-crystal x-ray diffraction structures of covalent organic frameworks. *Science* **361**, 48-52, (2018).

Acknowledgments

We thank Prof. V. Ferguson and A. Tomaschke for the nano-indentation test, Prof. D. Gin for the assistant on PXRD facility, Dr. B. Lama for ssNMR measurement, and X. Tang for CD measurement. The authors thank the University of Colorado Boulder and K. C. Wong Education Foundation for funding support. Y. C. gratefully acknowledges support from the National Science Foundation of China (91856204), Key Project of Basic Research of Shanghai (18JC1413200). W. G. is supported by the China Postdoctoral Science Foundation (2019M661482). X. C. is supported by the National Natural Science Foundation of China (No. 61925504). This research used resources of the Advanced Light Source, which is a DOE Office of Science User Facility under contract no. DE-AC02-05CH11231.

Author contributions

Y.H., Y.J., and W.Z. conceived the idea and lead the project. Y.H., H.C., and J.W. conducted the synthesis and crystal growth. W.G., Y.C., and S.T. carried out single crystal study and structure refinement. Z.Z., T.J., and X.C. performed AFM test and IR s SNOM measurements. Y.J. and W.Z. wrote the manuscript with help from Y.H. and Y.C. All the authors discussed and revised the manuscript.

Competing interests

The authors declare no competing interests.